Z. Phys. C - Particles and Fields 55, 307–315 (1992)

Zeitschrift für Physik C Particles and Fields

Relativistic effects and the constituent quark model of heavy quarkonia

M. Beyer, U. Bohn, M.G. Huber, B.C. Metsch, J. Resag

Institut für Theoretische Kernphysik, Nußallee 14–16, W-5300 Bonn, Federal Republic of Germany

Received 6 February 1992

Abstract. Charmonium $c\bar{c}$ and bottomonium $b\bar{b}$ are investigated in the framework of a constituent quark model. A scalar confining and a one-gluon exchange (OGE) potential are used in a nonrelativistic reduction to order $(p/m)^2$. Therefore the model includes spin dependent as well as spin independent terms. Their influence on the meson mass spectra and decay widths is analysed. We find that the experimental spectra can be reproduced by using a full model as well as by using a reduced version neglecting the spin independent terms. For both versions we calculate leptonic and radiative decay widths including relativistic corrections for the current operators. We find that for leptonic decays inclusion of all terms of the OGE potential gives better results than the non-relativistic formulas. For radiative transitions relativistic corrections are important.

1 Introduction

Since the discovery of J/ψ- [1] and Υ-resonances [2] many models have been studied to relate the spectra of charmonium $c\bar{c}$ and bottomonium $b\bar{b}$ to the underlying quark-antiquark ($q\bar{q}$) structure. Among them non-relativistic models [3–11] have been particularly successful in describing the mass spectra. This is mostly due to the fact that the masses of the constituents are relatively large. Those models lead to very similar results, since for $0.1\text{ fm} < r < 1\text{ fm}$, which is the typical scale for $c\bar{c}$ and $b\bar{b}$ mesons the various $q\bar{q}$ potentials used are nearly identical. For recent reviews see [12, 13] and references therein.

The various models however differ both in the long-range part and the short-range part of $q\bar{q}$ potential. The long-range part is responsible for the confinement of quarks. Since the problem of confinement has not yet been solved one has to rely on phenomenology for a reasonable ansatz. Results from lattice QCD as well as the Regge trajectories in light meson spectroscopy and their interpretation in terms of the flux tube model suggest a linear confining potential see e.g. [6]. The short-range part should reflect the concept of asymptotic freedom, which in most models is realized by one-gluon exchange (OGE). In early modeling, a short-range Coulomb-like $1/r$-potential was used [3, 4], which later was modified e.g. by taking into account that α_s is a running coupling constant [7]. Alternatively, the central potential has been approximated altogether by a logarithmic potential [5].

In addition, these models have to account for the spin-dependence of the $q\bar{q}$ interaction as reflected by the mass splitting of the spin triplet states χ_{cJ}, χ_{bJ} $(J=0, 1, 2)$ and in the hyperfine splitting of η_c and J/ψ. In the framework of OGE this can be done in a straightforward manner: A non-relativistic expansion in powers of p/m leads in addition to the $1/r$-potential in lowest order to spin dependent terms in next order. Note, that it also leads to spin independent terms in the same order. In analogy to QED the sum of all these terms will be referred to as Fermi-Breit interaction. This model leads to a reasonable agreement with experimental data (see also next section).

Nevertheless, the spin dependent terms alone yield mass splittings, that are already in quite good agreement with experiment. In the past this reduced version has been used in most of the quark models describing heavy quarkonia. For comparison, we therefore use both versions to investigate decay and transition observables, which are much more sensitive to details of the wave function than the spectra alone.

In Sect. 2 the model is introduced and the resulting mass spectra are shown. In Sect. 3 we calculate leptonic decay widths, E1- and M1-transition rates and investigate various approximations of the transition operators. Our results are discussed in Sect. 4.

2 The quark model

In the constituent quark model presented here, charmonium and bottomonium are treated as quark-antiquark states, i.e. we do not take into account any gluonic admixtures, which, presumably, should be small. Also no coupled channel effects are included although these might be relevant [4].

Confinement is implemented by a potential $\mathscr{V}_C$ assumed to a Lorentz scalar and thus giving rise to a Darwin and a Thomas precession term in addition to a linear confining potential. Furthermore, we assume that there is a residual short-range quark interaction from one-gluon-exchange $\mathscr{V}_R$. A nonrelativistic reduction of these interactions is done up to order $(p/m)^2$ as explained in the following.

Spectra and wave functions are obtained by solving the Schrödinger equation with the hamiltonian given by [13]

$$H = M + T + \mathscr{V}_C + \mathscr{V}_R \tag{1}$$

where M is the sum of the constituent quark masses, $m_q = m_{\bar{q}} = m$, and T the kinetic energy of relative motion in the center of mass system. We define the potential through $\mathscr{V} = V + W$, where W denotes the order $(p/m)^2$ and V the lower orders in a p/m expansion, for confining and residual interactions, respectively. For the lowest order in p/m the $q\bar{q}$-interactions read

$$V_C = a + br \tag{2}$$

$$V_R = -\frac{4}{3}\alpha_s \frac{1}{r}. \tag{3}$$

The terms of order $(p/m)^2$ are given by

$$W_C = W_C^{LS} + W_C^{Da} \tag{4}$$

$$W_R = W_R^{SS} + W_R^{LS} + W_R^{T} + W_R^{LL} + W_R^{Da} \tag{5}$$

They are sorted according to their spin dependence, viz. spin-spin, spin-orbit, tensor, Darwin, and orbit-orbit interaction, in obvious notation. The explicit forms are given by

$$W_C^{LS} = -\frac{1}{2m^2}\mathbf{L}\cdot\mathbf{S}\frac{1}{r}V_C' \tag{6}$$

$$W_C^{Da} = -\frac{1}{4m^2}(2\mathbf{p}^2 V_C + 2V_C\mathbf{p}^2 + \Delta V_C) \tag{7}$$

$$W_R^{SS} = \frac{2}{3m^2}\mathbf{s}_q\cdot\mathbf{s}_{\bar{q}}\Delta V_R \tag{8}$$

$$W_R^{LS} = \frac{2}{3m^2}\mathbf{L}\cdot\mathbf{S}\frac{1}{r}V_R' \tag{9}$$

$$W_R^{T} = \frac{1}{3m^2}S_{q\bar{q}}\left(\frac{1}{r}V_R' - V_R''\right) \tag{10}$$

$$W_R^{LL} = \frac{1}{8m^2}\left[2\mathbf{p}^2(V_R - rV_R') + 2(V_R - rV_R')\mathbf{p}^2 + \Delta(3V_R - rV_R') + 4\mathbf{L}^2\frac{1}{r}V_R'\right] \tag{11}$$

$$W_R^{Da} = \frac{1}{4m^2}\Delta V_R. \tag{12}$$

In the above expressions, $\mathbf{r}$ denotes the relative distance between quark and antiquark, $\mathbf{s}_q$ and $\mathbf{s}_{\bar{q}}$ are the respective spins ($\mathbf{s}_q = \boldsymbol{\sigma}_q/2$), $\mathbf{S} = \mathbf{s}_q + \mathbf{s}_{\bar{q}}$ the total spin, $S_{q\bar{q}} = 3\mathbf{s}_q\cdot\hat{\mathbf{r}}\,\mathbf{s}_{\bar{q}}\cdot\hat{\mathbf{r}} - \mathbf{s}_q\cdot\mathbf{s}_{\bar{q}}$ the tensor operator, and $\mathbf{L}$ is the relative angular momentum. The quark masses, and the parameters of the potentials, the off-set a, the string tension b and the coupling strength α_s are treated as free parameters which are adjusted to reproduce the experimental meson spectrum. Values are shown in Table 1. They are given for two different model versions: All terms of (4) and (5) included in the hamiltonian will be denoted as version A, and spin independent terms neglected, viz. $W_C^{Da} = W_R^{LL} = W_R^{Da} = 0$, will be denoted as version B.

Given the particular from of V_R as in (2) and (3), note that through derivatives, the terms of W_R diverge stronger than $1/r^2$ for $r \to 0$. If these terms are attractive, as they are e.g. for the scalar and pseudoscalar mesons through spin-orbit and spin-spin interactions, the mesons collapse, viz. the hamiltonian H is unbound from below. This is despite the kinetic energy term that is proportional to p^2 and would cure divergencies of lower order. Therefore the divergent terms are usually treated perturbatively. On the other hand, it has been argued [14] that these divergences are spurious due to the nonrelativistic reduction and should vanish, if all higher order corrections of (p/m) could be included. Since we do not use a pertubative treatment, we therefore need to regularize the potentials. This will be done in a way that keeps the terms of OGE dominant at small distances to model the concept of asymptotic freedom. Thus, not only the residual OGE but also the confining potential needs regularization. The latter would give a $1/r$ singularity in the spin-orbit term W_C^{LS} otherwise. We chose

$$1/r \to \sum_{i=1}^{5}\beta_i \exp[-\gamma_i^2 r^2], \tag{13}$$

for the residual interaction V_R and in the confining potential we replace

$$b \to b(r) = b\cdot(1 - \exp[-(r/2r_0)^2]). \tag{14}$$

The parameters β_i and γ_i are fixed to fit $1/r$ with maximum likelihood in the region between r_0 and $4r_0$, which is the relevant region for charmonium and bottomonium. The regularization scale r_0 is a free parameter of the model and its value is also shown in Table 1. Its inverse is in the order of the constituent quark mass m and may be interpreted as an effective size of the constituent quark. The regularized lowest order potential $V(r)$ is shown in Fig. 1 and compared with the nonregularized one. In fact, to be a reasonable regularization, mass spectra should not be too sensitive to a variation of r_0. This is indeed the case for $0.1\text{ fm} \lesssim r_0 \lesssim 0.25\text{ fm}$.

In passing, we note that mainly due to this regularization the parameter α_s should not be mistaken for the coupling constant of QCD. In our model α_s is of rather phenomenological character.

Table 1. Parameters entering the hamiltonian for the full model (version A) and the reduced model (version B)

parameter		version A	version B
m_c	[GeV]	1.907	2.344
m_b	[GeV]	5.306	5.690
a	[GeV]	−0.864	−1.495
b	[GeV/fm]	0.740	0.637
α_s		0.474	0.503
r_0	[fm]	0.14	0.18

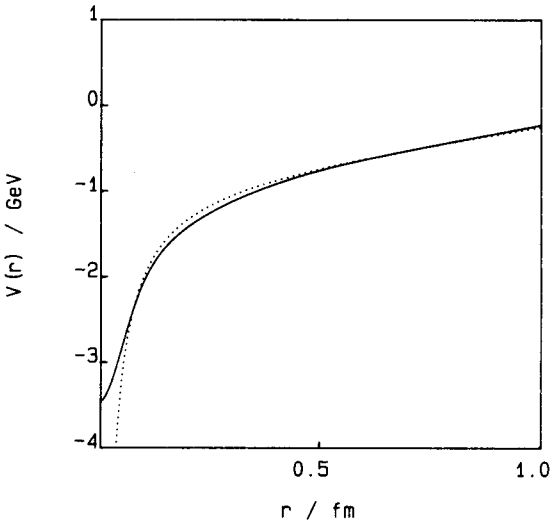

Fig. 1. Lowest order central potential $V(r)=V_R(r)+V_C(r)$ using the parameters of version A as given in Table 1. The dotted curve corresponds to the unregularized potential, while the solid curve corresponds to the regularized one

Table 3. Rms-radii given in fm for various mesons

R_{rms}	version A	version B
η_c	0.36	0.29
J/ψ	0.42	0.34
ψ'	0.83	0.73
ψ''	0.84	0.72
ψ'''	1.16	1.05
χ_{c0}	0.53	0.45
χ_{c1}	0.63	0.53
χ_{c2}	0.66	0.57
η_b	0.20	0.19
Υ	0.22	0.21
Υ'	0.49	0.47
Υ''	0.73	0.72
Υ'''	0.93	0.87
χ_{b0}	0.34	0.33
χ'_{b0}	0.60	0.59
χ_{b1}	0.36	0.35
χ'_{b1}	0.63	0.61
χ_{b2}	0.38	0.36
χ'_{b2}	0.65	0.62

The regularized hamiltonian is then diagonalized in a reasonably large basis of oscillator wave functions. In fact, our results do not change significantly, when the basis is enlarged or reduced. This choice of basis states and regularization scheme enables us to calculate the various matrix elements analytically.

The energy eigenvalues of the two versions are obtained by minimizing the expectation value with respect to the oscillator parameter of the wave functions due to Ritz' variational principle. The parameters are determined by a χ^2 fit of the energy eigenvalues to the experimental mass spectrum.

The mass spectra obtained with the best fit parameters as given in Table 1 are depicted in Fig. 2.

Both versions give a reasonable description of the experimental mass spectra, for charmonium as well as for bottomonium. The contributions of the various potentials to the total energy of some selected mesons are shown in Table 2. Note, that the spin independent terms W_R^{LL}, W_R^{Da}, W_C^{Da}, which are neglected in version B, lead to rather large expectation values. Nevertheless, version B still reproduces the experimental spectra due to readjustment of the parameters as is seen in Table 1. In particular, the off-set parameter a is changed by almost a factor of two.

As can also be seen from Table 2, the net effect of the spin independent terms is repulsive, with the largest contributions from W_C^{Da}-part. As a consequence, the mesons of the full model are larger than those in version B, which is shown in Table 3. In addition these terms reduce the effect of the short-range spin dependent terms, which are responsible for the spin splittings in the reduced version. The spin independent terms in the full model counteract the splittings due to the spin dependent terms W_R^{SS} and W_R^{LS}. This is reflected in the quark masses, which enter the spin dependent terms as a factor $1/m^2$. They are smaller for the full model than for the reduced version. And since relativistic effects are less important for bottomonium ($m_b > m_c$) the difference is less (8%) than in charmonium (20%).

3 Electromagnetic transitions and decays

It has been seen in the preceding section that despite differences in details both versions considered here lead to an equally good description of the experimental mass spectra. We now calculate leptonic decays and electromagnetic (E1, M1) transitions that should serve as more

Table 2. Expectation values in MeV for the terms contributing to W_C and W_R

Meson	version A							version B			
	SS	LS_R	LS_C	T	Da_R	LL_R	Da_C	SS	LS_R	LS_C	T
η_c	−136	–	–	–	68	−98	168	−141	–	–	–
J/ψ	16	0	0	−4	24	−44	95	21	0	0	−3
χ_{c0}	4	−200	23	–	6	−109	207	4	−151	14	–
χ_{c1}	1	−32	9	–	1	−36	92	1	−37	6	–
χ_{c2}	0	22	−8	–	1	−28	74	0	25	−6	–
η_b	−69	–	–	–	34	−61	77	−50	–	–	–
Υ	15	0	0	−1	23	−42	59	13	0	0	0
χ_{b0}	1	−60	4	–	2	−37	65	1	−49	3	–
χ_{b1}	1	−21	2	–	1	−26	51	1	−20	1	–
χ_{b2}	0	17	−2	–	1	−21	44	0	16	−1	–

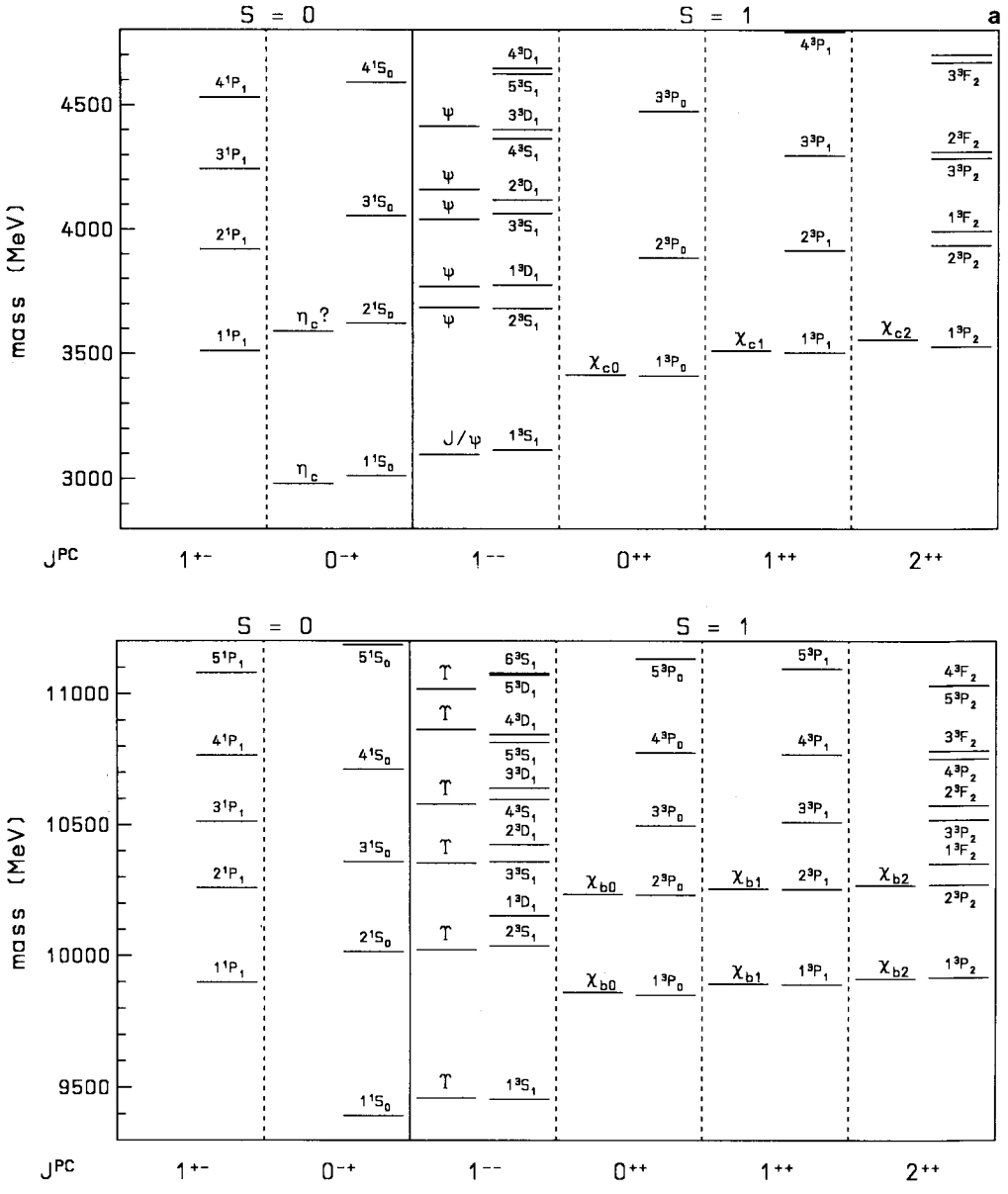

Fig. 2. a Meson mass spectrum. Left part of each column experiments [20]. Right part of each column as calculated in version *A*. Upper part charmonium, lower part bottomonium

sensitive tests of the details of the potentials, in particular the influence of the spin-independent residual interactions.

To this end it is necessary to define a Fock-space representation for the mesons. This has been done e.g. by van Royen and Weisskopf [16] and by Godfrey and Isgur [15], and we follow their procedure with minor changes.

As in [15] the meson is represented by a superposition of free quark-states $|\mathbf{p}\rangle = a^+(\mathbf{p})|0\rangle$ (or $b^+(\mathbf{p})|0\rangle$ for the antiquark) and the amplitudes given by the nonrelativistic meson wave function in momentum space

$$|\omega \mathbf{P}\rangle = \sqrt{2\omega}\int \frac{d^3p}{(2\pi)^3}\frac{1}{\sqrt{2p_q^0\,2p_{\bar{q}}^0}}\sum_L R_{NL}(p) \cdot [Y_L(\hat{p})\otimes\chi^S]^J \chi^F \chi^C |\tfrac{1}{2}\mathbf{P}+\mathbf{p}\rangle_q |\tfrac{1}{2}\mathbf{P}-\mathbf{p}\rangle_{\bar{q}} \qquad (15)$$

where $\mathbf{p}_q$, $\mathbf{p}_{\bar{q}}$ are the quark momenta, $p_q^0 = \sqrt{\mathbf{p}_q^2 + m^2}$ (and analogously for $\bar{q}$) the free quark energies, $\mathbf{P} = \mathbf{p}_q + \mathbf{p}_{\bar{q}}$ the total momentum, $\mathbf{p} = (\mathbf{p}_q - \mathbf{p}_{\bar{q}})/2$ the relative momentum of the two quarks which are normalized as $\langle \mathbf{p}_q | \mathbf{p}_q' \rangle = (2\pi)^3 2p_0 \delta(\mathbf{p}_q - \mathbf{p}_q')$. The spin, flavor, and color wave functions are given by χ^S, χ^F, χ^C, resp. The momentum space relative wave function is denoted by $R_{NL}(p)\, Y_{LM}(\hat{p})$. With μ the experimental meson mass, $\omega = \sqrt{\mathbf{P}^2 + \mu^2}$ is the energy of the meson. Thus the normalization chosen in (15) is a different choice as [15], viz. $\langle \mathbf{P}_q | \mathbf{P}_q' \rangle = (2\pi)^3 2\omega \delta(\mathbf{P}_q - \mathbf{P}_q')$. For other normalizations, see [15].

We will not make the approximation $p/m = 0$ in the decay formulas, which will be given in the following, i.e. we do not neglect the small components of the Dirac spinors of quarks, when calculating S-matrix elements. Our formulas are then compared with the nonrelativistic approach, e.g. the well-known $|\psi(0)|^2$-formula (van Royen–Weisskopf-formula). Through comparison, we are then able to estimate the influence of relativistic effects in mesonic decays. One might interpret these effects as

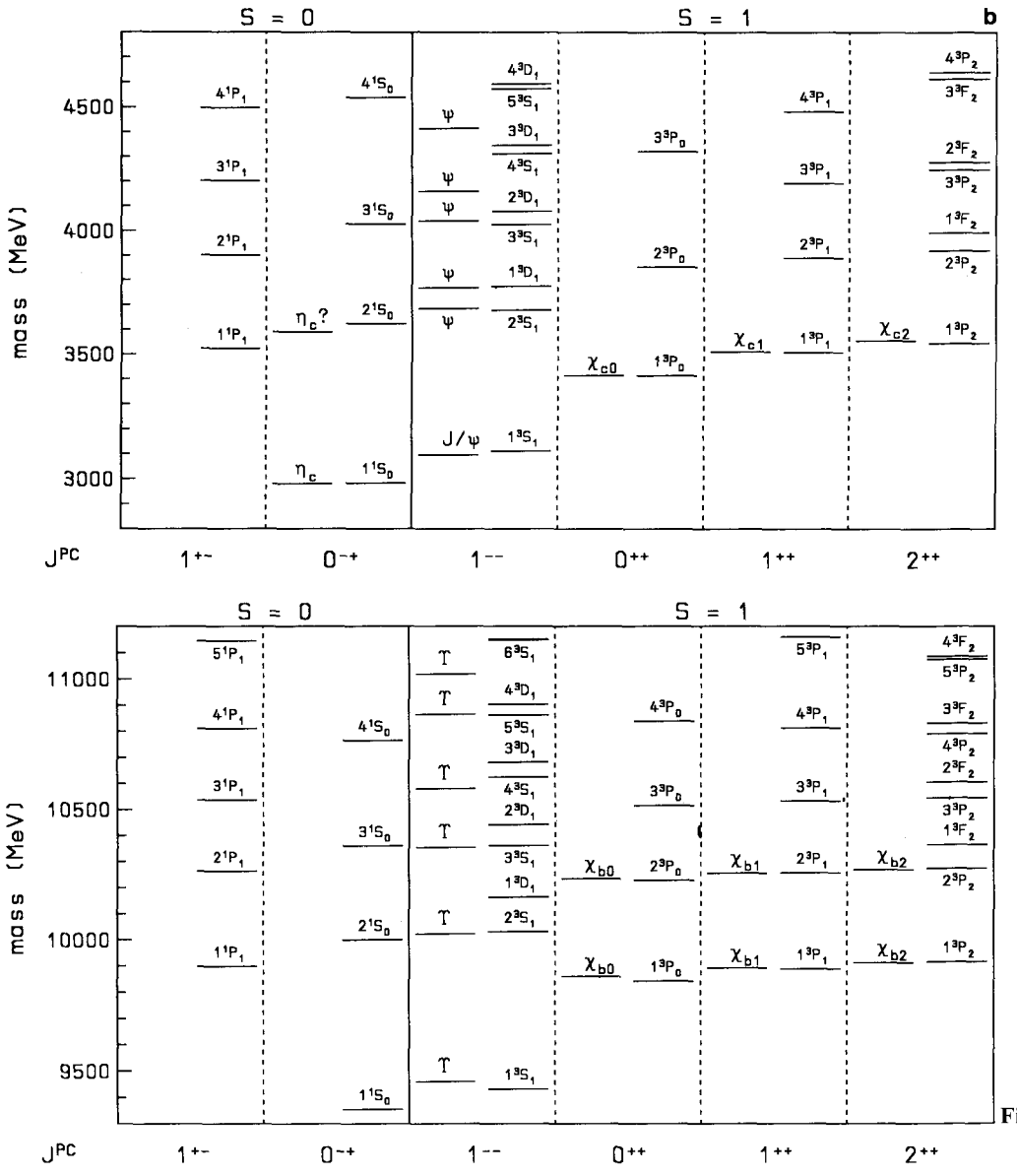

Fig. 2. b Same as **a** for version *B*

a smearing of the space coordinates of the quarks. In other words, $|\psi(0)|^2$ formulas are modified, since quarks can annihilate even if they are not at the same position, e.g. in an $L \neq 0$-state. We consider this a 'quasirelativistic' treatment.

Although this approach is not a covariant formalism, it is a natural way to include relativistic effects into the calculation of decays in a nonrelativistic quark model. The formalism should account for these effects in a proper way for charmonium and bottomonium, since p/m is small in these mesons.

We now consider *leptonic decays*, which is the inverse process of meson production in electron-positron annihilation. Due to selection rules, only the vector-mesons ($J^{PC}=1^{--}$) can be produced or decay via this channel. Therefore, the spin of the meson has to be $S=1$, however, the angular momentum can be $L=0$ or 2. Since the masses of electrons or muons are much smaller than the meson masses (we do not consider decays into τ-leptons), the decay width becomes independent of the lepton masses. We compare the following two formulas:

- The quasirelativistic formula as explained above is given by

$$\Gamma_{\text{lep}} = \frac{16\pi\alpha^2 e_q^2}{\mu^2} 4\pi \left(\int \frac{p^2 \mathrm{d}p}{(2\pi)^3} R_{NL=0}(p) \frac{2p^0 + m}{3p^0} + \int \frac{p^2 \mathrm{d}p}{(2\pi)^3} R_{NL=2}(p) \frac{2\sqrt{2}}{3\sqrt{3}} \frac{p^0 - m}{2p^0} \right)^2 \tag{16}$$

with $\alpha = 1/137$ and the quark charge e_q being 2/3 for the c-quark and $-1/3$ for the b-quark. Note, that this formula explicitly allows for decay of D-waves into leptons!

- The nonrelativistic formula, obtained by using $p/m = 0$

in (16) is given by

$$\Gamma_{\text{lep}}=\frac{16\pi\alpha^2 e_q^2}{\mu^2}|\psi(0)|^2 . \tag{17}$$

The D-wave-term vanishes and the momentum integral of the S-wave-term is equal to the spatial wave function at the origin $r=0$.

We now turn to radiative transitions. Some difficulty arises related to the proper boost of the final state meson, being a composed object. However, due to the small momenta involved, it is possible to neglect momentum of the final state and treat the decays in the long wavelength limit.

For *E1 transitions*, the transition width is given by the formula

$$\Gamma_{\text{E1}}=\tfrac{4}{3}\alpha e_q^2 k^3(2J'+1)\cdot\left\{\sum_{L,L'}(-1)^l\sqrt{l}\begin{Bmatrix}J' & L' & S\\ L & J & 1\end{Bmatrix}M_{fi}(\text{E1})\delta_{L'L\pm1}\delta_{SS'}\right\}^2 \tag{18}$$

where J, L, S belong to the initial meson and J', L', S' to the final meson, and $l=\max(L, L')$. We use the experimental photon energy for k in our calculation. The matrix element M_{fi} will be given in impulse approximation only.

- The quasirelativistic formula is obtained including the lower component of the quark Dirac spinors as explained in the beginning of the section and the long wavelength limit $k\ll p$.

$$M_{fi}(\text{E1})=\frac{2}{k}\int_0^\infty\frac{p^2\mathrm{d}p}{(2\pi)^3}R^f_{N'L'}(p)\frac{p}{p^0}R^i_{NL}(p) \tag{19}$$

- The nonrelativistic limit of the above formula leads to the following formula in *momentum* space

$$M_{fi}(\text{E1})=\frac{2}{k}\int_0^\infty\frac{p^2\mathrm{d}p}{(2\pi)^3}R^f_{N'L'}(p)\frac{p}{m}R^i_{NL}(p) \tag{20}$$

- If $\mathbf{p}=2m[H, \mathbf{r}]$ holds, the above *momentum* space formula is equivalent to the following *coordinate* space one

$$M_{fi}(\text{E1})=\frac{2}{k}\int_0^\infty r^2\mathrm{d}r R^f_{N'L'}(r)r R^i_{NL}(r) \tag{21}$$

However, (20) and (21) lead to different results, if the potential is momentum dependent, as is the case in our model. In fact, since we are working in the long-wavelength limit, (21) can be obtained by using *Siegert's theorem*. Thus the difference between (20) and (21) gives a hint for the validity of impulse approximation.

- Going beyond the long-wavelength limit an *extended* nonrelativistic formula in coordinate space reads [4].

$$M_{fi}(\text{E1})=\frac{3}{k}\int_0^\infty r^2\mathrm{d}r R^f_{N'L'}(r)\cdot\left\{\left(1+\frac{k}{4m}\right)(\tfrac{1}{2}kr j_0(\tfrac{1}{2}kr)-j_1(\tfrac{1}{2}kr))\pm\frac{k}{4m}(J(J+1)-4)j_1(\tfrac{1}{2}kr)+\frac{k}{2m}j_1(\tfrac{1}{2}kr)\frac{\partial}{\partial r}r\right\}R^i_{NL}(r) \tag{22}$$

where the plus sign holds for $S\to P$ transitions and the minus sign holds for $P\to S$. In the long-wavelength limit this formula reproduces formula (21).

The *M1 transition* widths are described by the formula

$$\Gamma_{\text{M1}}=\frac{4\alpha e_q^2}{3m^2}k^3(2J'+1)M^2_{fi}(\text{M1}) . \tag{23}$$

This formula is valid only for transitions with $\Delta S=1$ and $L=L'=0$. The small D-wave admixture is neglected. We compare three different formulas for the matrix element M_{fi}:

- The quasirelativistic formula in the approximation given before reads

$$M_{fi}(\text{M1})=\int_0^\infty\frac{p^2\mathrm{d}p}{(2\pi)^3}R^f_{N'0S'}(p)\frac{m^2+2mp^0}{3(p^0)^2}R^i_{N0S}(p) . \tag{24}$$

Due to the change of the total spin S an additional index S is used for the radial part of the wave function. In lowest nonrelativistic order this formula yields the following equation.

- The nonrelativistic formula

$$M_{fi}(\text{M1})=\int_0^\infty r^2\mathrm{d}r R^f_{N'0S'}(r)R^i_{N0S}(r)=\int_0^\infty\frac{p^2\mathrm{d}p}{(2\pi)^3}R^f_{N'0S'}(p)R^i_{N0S}(p) . \tag{25}$$

Models using undistorted wave functions not affected by residual interactions give $R^f_{N0S'}=R^i_{N0S}$ for the radial part of the wave functions yielding $M_{fi}(\text{M1})=\delta_{NN'}$ in (25). Therefore M1 transitions with $N\neq N'$ are expected to be strongly suppressed ('forbidden').

- Going beyond the long-wavelength limit the nonrelativistic formula reads

$$M_{fi}(\text{M1})=\int_0^\infty r^2\mathrm{d}r R^f_{N'0S'}(r)j_0(\tfrac{1}{2}kr)R^i_{N0S}(r) \tag{26}$$

The long-wavelength limit, $j_0\approx1$, leads to (25).

In order to qualitatively discuss the relativistic effects in the above formulas, we analyze the integrands involved in leptonic decays and M1 transition rates. If we neglect the D-wave term in (16), the difference between the two formulas (16) and (17) is given by the integrand

$$\mathcal{I}_{\text{lep}}(p^0)=\frac{2p^0+m}{3p^0} \tag{27}$$

which equals unity in the nonrelativistic limit. This function is plotted in Fig. 3. The integrand suppresses higher momenta, which corresponds to the fact that contributions of the wave function at very small distances becomes less important. However, typical values for p/m are 0.5 in charmonium and 0.25 in bottomonium, for which values the integrand is not very different from unity. Therefore these decays may provide a test to the wave function input, viz. the different versions of the model presented, since relativistic effects might (accidentally) be small in leptonic decays. Unfortunately, only the vector mesons

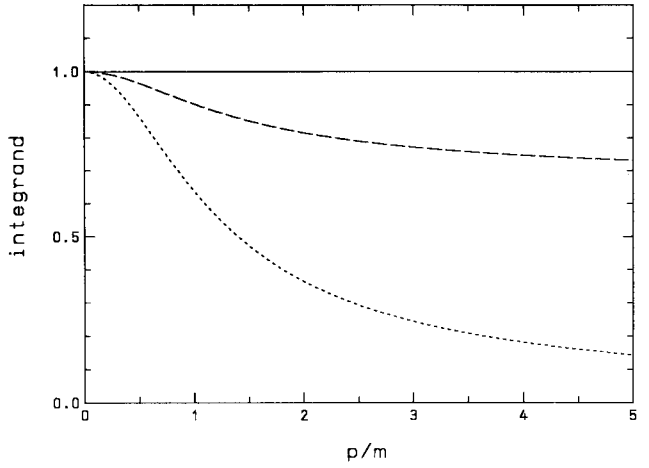

Fig. 3. Plot of the integrand $\mathcal{I}_{\text{lep}}$ (dashed curve) used in the S-wave part of the quasirelativistic leptonic decay formula (16) and the integrand $\mathcal{I}_{\text{M1}}$ (dotted curve) used in quasirelativistic M1 transition formula (24)

can be tested this way. For M1 transitions differences between the quasirelativistic and the nonrelativistic treatment are given by the following integrand

$$\mathcal{I}_{\text{M1}}(p^0)=\frac{m^2+2mp^0}{3(p^0)^2}. \tag{28}$$

A plot is shown in Fig. 3. From the figure we expect, that for typical value of charmonium and bottomonium as given above, relativistic corrections in the operators are more important here than for the leptonic decays.

4 Results

We find that relativistic corrections are necessary for a better description of heavy quarkonia. This is in agreement with [14].

In charmonium, the full and the reduced model version as presented in Sect. 2 give satisfactory results for the γ-transition rates. However, for leptonic decays, the full model much better describes the data. In addition the leptonic decay formulas are more reliable due to less approximations and less importance of relativistic corrections in the operators (see Fig. 3). We therefore favor the full model, which yields a better overall description.

Comparing calculated and experimental leptonic widths in detail, for the S-wave-states in charmonium (Table 4), we find that the data of version *B* are too large by a factor ~ 2 to 3, while the data of the full model are in quite good agreement with experiment. Relativistic corrections are of the order of 10%, improving the agreement with the experimental data. On the other hand, they are also small enough to ensure that the quasirelativistic treatment, as explained in Sect. 3, is reasonable. The differences between the two versions are dominated by the repulsive Darwin-terms, as see from Table 2.

The decay widths of the D-waves in charmonium are too small by more than one order of magnitude, but nonzero due to S-wave admixture by the tensor force and

Table 4. Leptonic decay widths given in keV: *a* using the full Dirac operator for quarks (16), *b* nonrelativistic approximation (17), $(\,)^d$ denotes mesons dominated by d-waves

decay	Γ_{exp}	version A		version B	
		a	*b*	*a*	*b*
$J/\psi(1S)\to l^+l^-$	4.72 ± 0.35	5.33	5.72	11.2	12.2
$\psi(2S)\to l^+l^-$	2.14 ± 0.21	2.31	2.62	4.06	4.63
$\psi(3770)^d\to l^+l^-$	0.26 ± 0.04	0.01	0.002	0.03	0.005
$\psi(4040)\to l^+l^-$	0.75 ± 0.15	1.59	1.85	2.74	3.20
$\psi(4160)^d\to l^+l^-$	0.77 ± 0.23	0.02	0.003	0.04	0.01
$\psi(4415)\to l^+l^-$	0.47 ± 0.10	1.14	1.35	2.06	2.41
$\Upsilon(1S)\to l^+l^-$	1.34 ± 0.04	1.24	1.32	1.41	1.49
$\Upsilon(2S)\to l^+l^-$	0.586 ± 0.029	0.51	0.55	0.56	0.61
$\Upsilon(3S)\to l^+l^-$	0.44 ± 0.03	0.35	0.38	0.36	0.39
$\Upsilon(4S)\to l^+l^-$	0.24 ± 0.05	0.28	0.31	0.30	0.33

relativistic effects (D-wave term in (16)). However, these particular decay width may be dominated by coupled channels and results may improve due to additional S-wave admixture [4].

In passing we mention some concerns about an additional one gluon QCD-correction factor of the form

$$\left(1-\frac{16}{3\pi}\alpha_s\right)\approx 0.3 \tag{29}$$

in analogy to corresponding QED-radiation-corrections used in positronium decays [4, 17, 18]. The use of this correction factor is not free of bias as discussed in [17], because the radiative correction to the quark-antiquark interaction has already been included in the potential. As we have shown, our results are in quite good agreement with experimental data without any correction of that kind.

For E1 transitions in charmonium we find that both hamiltonians (version A and B) lead to comparable results (Table 5). The results for the various approximations (19)–(22) show that also here the quasirelativistic formula (19) leads to quite good agreement with experiment. The relativistic effects are of the order of 20–30% and lead to a significant reduction of the corresponding nonrelativistic results of (20). Effects of the long-wavelength approximation (compare (21) to (22)) are generally much smaller and become important only for the transition $\chi_{c2}(1P)\to J/\psi(1S)\gamma$ with the largest photon momentum k. This is in agreement with results found by others [4, 14]. Coupled channel effects may further reduce the widths by 10–20%, and would thus lead to a good agreement with experiment [4].

We find that two body currents might play some role (compare columns *c* and *d* in Table 5), less so for bottomonium. In transitions that are close to the long wavelength limit, differences are not so large, and comparable to the differences emerging for the two model versions.

We emphasize that some E1 transitions are very sensitive to the nodes of the wave functions, which lead to large cancellations in the matrix elements. This explains the partly large differences in some decays using different formulas or the two models considered.

Table 5. E1 transition widths in keV for the full model (version *A*) and the reduced model (version *B*). Experimental data are taken from [20], † from [21]. *a*–*c* along wavelength limit: *a* using the full Dirac operator for quarks (19), *b* nonrelativistic approximation using momentum space formula (20), *c* nonrelativistic approximation using coordinate space formula (21). *d* same as *c* but without employing the long wavelength limit (22)

decay		experiment		version A				version B			
				a	*b*	*c*	*d*	*a*	*b*	*c*	*d*
$\psi'(2S)$	$\to \chi_{c0}(1P)\,\gamma$	22.6	±4.5	24.2	34.1	22.7	21.6	19.9	28.0	19.4	18.5
	$\to \chi_{c1}(1P)\,\gamma$	21.1	±4.2	31.3	43.9	47.6	45.6	27.3	38.2	34.8	33.7
	$\to \chi_{c2}(1P)\,\gamma$	19.0	±4.0	26.3	36.8	37.2	36.2	19.8	27.7	29.3	28.7
$\chi_{c0}(1P)$	$\to J/\psi(1S)\,\gamma$	92	±40	189	317	215	240	191	234	147	163
$\chi_{c1}(1P)$	$\to J/\psi(1S)\,\gamma$	240	±40†	264	315	438	447	262	315	287	297
$\chi_{c2}(1P)$	$\to J/\psi(1S)\,\gamma$	267	±33†	271	321	602	476	259	305	393	333
$\Upsilon(3S)$	$\to \chi_{b0}(2P)\,\gamma$	1.2	±0.4	1.18	1.38	1.00	1.00	1.06	1.23	1.00	0.99
	$\to \chi_{b1}(2P)\,\gamma$	2.9	±0.7	2.21	2.61	2.30	2.28	2.07	2.41	2.11	2.09
	$\to \chi_{b2}(2P)\,\gamma$	3.1	±0.8	2.29	2.70	2.80	2.78	2.26	2.62	2.59	2.57
$\Upsilon(2S)$	$\to \chi_{b0}(1P)\,\gamma$	1.9	±0.6	1.11	1.33	0.88	0.87	1.03	1.22	0.85	0.84
	$\to \chi_{b1}(1P)\,\gamma$	2.9	±0.7	1.88	2.25	1.83	1.81	1.83	2.15	1.64	1.63
	$\to \chi_{b2}(1P)\,\gamma$	2.9	±0.7	1.82	2.17	2.11	2.09	1.85	2.18	2.00	1.88
$\chi_{b0}(2P)$	$\to \Upsilon(2S)\,\gamma$			11.9	13.5	15.2	15.5	11.4	12.7	13.8	14.1
	$\to \Upsilon(1S)\,\gamma$			3.78	5.13	2.26	3.05	3.73	4.93	2.52	3.23
$\chi_{b1}(2P)$	$\to \Upsilon(2S)\,\gamma$			13.7	15.4	16.9	16.9	12.9	14.3	15.8	15.8
	$\to \Upsilon(1S)\,\gamma$			7.03	8.91	7.04	7.98	6.26	7.86	6.15	6.92
$\chi_{b2}(2P)$	$\to \Upsilon(2S)\,\gamma$			14.1	15.6	17.8	17.0	13.4	14.8	16.8	16.1
	$\to \Upsilon(1S)\,\gamma$			8.14	9.98	12.1	11.3	7.33	8.92	10.5	9.90
$\chi_{b0}(1P)$	$\to \Upsilon(1S)\,\gamma$			31.8	35.2	28.3	29.9	29.7	32.6	26.2	27.6
$\chi_{b1}(1P)$	$\to \Upsilon(1S)\,\gamma$			33.4	36.6	32.5	33.1	31.5	34.3	30.4	30.9
$\chi_{b2}(1P)$	$\to \Upsilon(1S)\,\gamma$			32.0	34.7	37.0	34.6	30.4	32.9	34.6	32.5

Table 6. M1 transition widths in keV for the full model (version *A*) and the reduced model (version *B*). Experimental data are taken from [20]. For charmonium experimental photon energies *k* have been used. For bottomonium photon energies are calculated from version *A* (version *B*), respectively, *a*, *b* long wavelength limit: *a* using the full Dirac operator for quarks (24), *b* nonrelativistic approximation (25), *c* same as *b* but without employing the long wavelength limit (26)

decay		experiment	version A			version B			$k\,[MeV]$
			a	*b*	*c*	*a*	*b*	*c*	
$\psi'(2S)$	$\to \eta_c(1S)\,\gamma$	0.7 ± 0.2	0.93	5.92	12.3	0.87	4.47	7.25	706
	$\to \eta_c(2S)\,\gamma$		0.81	0.99	0.97	0.27	0.66	0.65	96
$J/\psi(1S)$	$\to \eta_c(1S)\,\gamma$	0.9 ± 0.3	1.53	1.84	1.83	1.00	1.21	1.21	117
$\eta_c(2S)$	$\to J/\psi(1S)\,\gamma$		15.8	9.03	4.2	11.1	6.49	4.0	493
$\Upsilon(2S)$	$\to \eta_b(1S)\,\gamma$		0.018	0.063	0.094	0.006	0.027	0.043	668 (629)
$\Upsilon(1S)$	$\to \eta_b(1S)\,\gamma$		0.040	0.044	0.044	0.009	0.010	0.009	105 (66)
$\eta_b(2S)$	$\to \Upsilon(1S)\,\gamma$		0.225	0.124	0.082	0.135	0.065	0.038	540 (556)

For *M1 transitions*, we find that the quasirelativistic formula (24) always yields results closest to the experimental data. In fact, they are within the experimental errors for version *B* and slightly larger for the full model. Results are given in Table 6. Comparing different formulas we see that long-wavelength limit effects may be important for large *k*-values ($k \approx 700$ MeV) (column *b* compared to column *c* in Table 6), although they do not yield agreement with experiment. The well-known disagreement between the non-relativistic results of (25), (26) and experiment seems to be accommodated by including relativistic effects due to (24). Note, that no anomalous magnetic moment of the charmed quark needs to be introduced [14, 19] to resolve this long standing difficulty.

If we compare matrix elements of forbidden and allowed M1 transitions, we also find for our model that matrix elements with different N are smaller than those with equal N by about one order of magnitude. This shows that there are large cancellations in the matrix elements of forbidden decays. In particular, the matrix element for $2S \to 1S$ is very sensitive to the exact location of the node of the 2*S*-state, similar to some E1 transitions mentioned above. In Fig. 4 the wave functions of $\psi(2S)$ and $\eta_c(1S)$ are shown to demonstrate this issue. For this reason the matrix element is also sensitive to changes of the integrand (i.e. relativistic corrections in the transition operators), which results in a significant reduction of the width of this forbidden transition.

In bottomonium we find that both versions (*A* and *B*) lead to reasonable overall agreement with leptonic decay as well as transition data. The differences in the various approximations turns out to be smaller here, because the spin-independent forces are reduced by a factor $1/m^2$. As expected, the relativistic corrections are smaller due to the smaller fraction of $(p/m)^2 \approx 6\%$ in bottomonium.

In more detail, in bottomonium the $3S \to 2P$-transitions are in good agreement with experiment, while the $2S \to 1P$-transitions are slightly too small. The fractions $(2P \to 2S)/(2P \to 1S)$ are in agreement with the experimental fractions, too. The differences between various decay formulas are smaller than for charmonium. We emphasize that the $1P \to 1S$-transitions are not affected by the exact location of the nodes. Unfortunately, up to now the total widths of the χ_b's have not been measured.

Since the total decay width of $\chi_b(2P)$ mesons is not known experimentally, we have given the ratios for some decays in Table 7. Experimental errors are assumed to be statistical. We find that all variations are congruent with experimental data.

Table 7. Ratios for selected decays in bottomonium. Experimental ratios calculated from [20] assuming statistical errors only. Letters assigned as in Table 5

decay ratio	experiment	version A				version B			
		a	*b*	*c*	*d*	*a*	*b*	*c*	*d*
$\chi_{b0}(2P)$: $\Gamma(\Upsilon(2S)\,\gamma)/\Gamma(\Upsilon(1S)\,\gamma)$	5.0 ±4.5	3.1	2.6	6.7	5.1	3.1	2.6	5.5	4.4
$\chi_{b1}(2P)$: $\Gamma(\Upsilon(2S)\,\gamma)/\Gamma(\Upsilon(1S)\,\gamma)$	4.1 ±1.7	1.9	1.7	2.4	2.1	2.1	1.8	2.6	2.3
$\chi_{b2}(2P)$: $\Gamma(\Upsilon(2S)\,\gamma)/\Gamma(\Upsilon(1S)\,\gamma)$	3.0 ±1.4	1.7	1.6	1.5	1.5	1.8	1.7	1.6	1.6

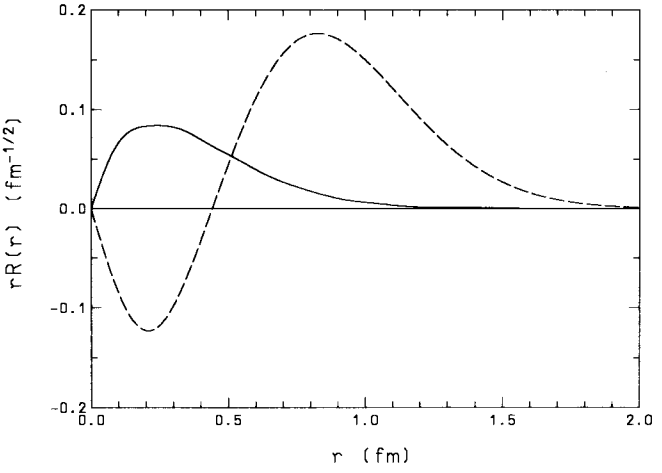

Fig. 4. Radial densities $r\,R_{NOS}(r)$ for $\psi(2S)$ (dashed curve) and $\eta_c(1S)$ (solid curve) using the parameters of the full model

5 Conclusion

For the binding of quark and antiquark we use a non-relativistically reduced version of the OGE potential and a confining potential assumed to be of Lorentz scalar nature. The spin dependent terms occurring in order $(p/m)^2$ are important to account for the various spin splittings in the meson mass spectra. For a systematic approach, we also include the spin independent terms and relativistic corrections of the transition operators.

For the mass spectra, we find that the spin independent terms and the spin dependent terms give contributions to the masses of the same order of magnitude. Nevertheless, both versions, the full model (version *A*) and a reduced version with spin independent terms neglected (version *B*), yield a meson mass spectrum of similar quality. The effects of the spin independent terms in the full model can be largely compensated for by a change of parameters in version *B*.

We find that leptonic decay widths are more sensitive to the particular potential input, due to smaller relativistic effects, than the γ transition rates. Since they are better described in the full model, we favor version *A*. From the resulting E1 transition rates we conclude that also two body contributions to the current operators may be of some relevancy.

The presented calculational scheme provides an improved description of heavy quarkonia [22]. Nevertheless, the magnitude of relativistic corrections found in this noncovariant approach, actually implies that a genuine relativistic treatment of quarkonia might be relevant. This of course applies a forteriori to the light mesonic systems.

References

1. J.J. Aubert et al.: Phys. Rev. Lett. 33 (1974) 1404; J.-E. Augustin et al.: Phys. Rev. Lett. 33 (1974) 1406
2. S.W. Herb et al.: Phys. Rev. Lett. 39 (1977) 252
3. A. De Rújula, H. Georgi, S.L. Glashow: Phys. Rev. D 12 (1975) 147
4. E. Eichten et al.: Phys. Rev. D 17 (1978) 3090; D 21 (1980) 203
5. C. Quigg, J.L. Rosner: Phys. Lett. 21B (1977) 153
6. W. Kwong, J.L. Rosner, C. Quigg: Ann. Rev. Nucl. Part. Sci. 37 (1987) 325
7. W. Celmaster, H. Georgi, M. Machazek: Phys. Rev. D 17 (1978) 879
8. G. Bhanot, S. Rudaz: Phys. Lett. 78B (1978) 119
9. J. Richardson: Phys. Lett. 82B (1979) 272
10. W. Buchmüller, S.-H. Tye: Phys. Rev. D 24 (1981) 132
11. A. Martin: Phys. Lett. 93B (1980) 338
12. D.B. Lichtenberg: Int. J. Mod. Phys. A 2 (1987) 1669
13. W. Lucha, F.F. Schöberl, D. Gromes: Phys. Rep. 200 (1991) 127
14. R. McClary, N. Byers: Phys. Rev. D 28 (1983) 1692
15. S. Godfrey, N. Isgur: Phys. Rev. D 32 (1985) 189
16. R. Van Royen, V.F. Weisskopf: Nuovo Cimento 50, 2A (1967) 617
17. S.N. Gupta, S.F. Radford, W.W. Repko: Phys. Rev. D 26 (1982) 3305, D 31 (1985) 160
18. R. Barbieri, R. Gatto, R. Kögeler, Z. Kunszt: Phys. Lett. 57B (1975) 455
19. G.A. Miller, P. Singer: Phys. Rev. D 37 (1988) 2564
20. Particle Data Group: Phys. Lett. B239 (1990) 1
21. T.A. Armstrong et al.: FNAL Pub-91/213-E [Nucl. Phys. B (to be published)]; K.K. Seth: private communication
22. J. Resag: diploma thesis Bonn, unpublished